



HAL
open science

Comparison of Numerical Error Estimators for Eddy-Current Problems Solved by FEM

R. Tittarelli, Y. Le Menach, F. Piriou, Emmanuel Creusé, Serge Nicaise, J.-P.
Ducreux

► **To cite this version:**

R. Tittarelli, Y. Le Menach, F. Piriou, Emmanuel Creusé, Serge Nicaise, et al.. Comparison of Numerical Error Estimators for Eddy-Current Problems Solved by FEM. IEEE Transactions on Magnetics, 2018, 54 (3), pp.1-4. 10.1109/TMAG.2017.2736601 . hal-01947267

HAL Id: hal-01947267

<https://hal.science/hal-01947267v1>

Submitted on 20 Nov 2024

HAL is a multi-disciplinary open access archive for the deposit and dissemination of scientific research documents, whether they are published or not. The documents may come from teaching and research institutions in France or abroad, or from public or private research centers.

L'archive ouverte pluridisciplinaire **HAL**, est destinée au dépôt et à la diffusion de documents scientifiques de niveau recherche, publiés ou non, émanant des établissements d'enseignement et de recherche français ou étrangers, des laboratoires publics ou privés.

Comparison of Numerical Error Estimators for Eddy-Current Problems Solved by FEM

R. Tittarelli^{1,2}, Y. Le Menach², F. Piriou², E. Creusé¹, S. Nicaise³, J.-P. Ducreux⁴

¹Laboratoire Paul Painlevé, CNRS, UMR 8524, University Lille, F-59000 Lille, France

²L2EP, Centrale Lille, Arts et Métiers Paris Tech, University Lille, F-59000 Lille, France

³LAMAV Laboratory of Mathematics, University de Valenciennes, 59313 Valenciennes, France

⁴EDF-Research and Development (ERMES), 92120 Palaiseau, France

In the domain of field computation with the finite-element method, choosing the mesh refinement is an important step to obtain an accurate solution. In order to evaluate the quality of the mesh, a posteriori error estimators are frequently used. In this paper, we propose to analyze and to compare residual and equilibrated error estimators for eddy-current problems in the case of \mathbf{A} - φ and \mathbf{T} - Ω formulations. The different properties of the estimators will be discussed.

Index Terms—Electromagnetic fields, error estimation, finite-element analysis, harmonic analysis.

I. INTRODUCTION

THE finite-element method is widely used to solve eddy-current problems. Today, one of the challenges is to evaluate the quality of the solution with the help of error estimators. Some of them [1]–[3] based on a *posteriori* error analysis give an estimate of the spatial error distribution that can be used in the remeshing step.

In order to set up an adaptive mesh refinement, an error estimator must be reliable and (locally) efficient [1]–[3]. In the family of a *posteriori* error estimators the residual type can be used. In the case of magnetodynamic harmonic formulation, the reliability and the local efficiency have been proven [4] for two residual estimators. Their drawback is that the gap between the error and the estimator is unknown. A way to handle it consists in using equilibrated a *posteriori* error estimators built from the property of non-verification of equilibrium equations [5]. They give the spatial error distribution too and, in addition, provide very sharp and global error bounds.

In this paper, we present residual and equilibrated error estimators for eddy-current problems solved with \mathbf{A} - φ and \mathbf{T} - Ω harmonic formulations. A residual estimator is proposed for each of them. In the case of the equilibrated error estimator two approaches are proposed to determine the admissible fields [5]. As example of application these estimators are used to evaluate the quality of solution in the case of a coil between two conductive plates. The results given by each estimator are compared and discussed.

II. NUMERICAL MODELS

A. Studied Structure

Let us consider a domain \mathcal{D} of boundary Γ_B , as shown in Fig. 1. \mathcal{D} is divided into three subdomains: \mathcal{D}_s with the source term corresponding to the current density \mathbf{J}_s ; \mathcal{D}_c is

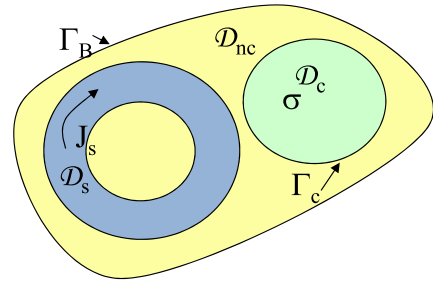


Fig. 1. Studied structure.

the conducting part; and \mathcal{D}_{nc} is the non-conducting one. The boundary condition on Γ_B is $\mathbf{B} \cdot \mathbf{n} = 0$ with \mathbf{B} the magnetic flux density and \mathbf{n} the unit normal vector. Similarly the boundary condition on Γ_c is $\mathbf{H} \wedge \mathbf{n} = 0$ with \mathbf{H} the magnetic field. To study our problem both well-known \mathbf{A} - φ and \mathbf{T} - Ω formulations will be considered.

B. Electric Formulation

For the \mathbf{A} - φ formulation from Maxwell's equations with the boundary condition on Γ_B , the weak formulation can be written as [6]

$$\begin{aligned} (\mu^{-1} \mathbf{curl} \mathbf{A}, \mathbf{curl} \mathbf{A}')_{\mathcal{D}} + (\sigma (j\omega \mathbf{A} + \mathbf{grad} \varphi), \mathbf{A}')_{\mathcal{D}_c} &= (\mathbf{J}_s, \mathbf{A}')_{\mathcal{D}} \\ (\sigma (j\omega \mathbf{A} + \mathbf{grad} \varphi), \mathbf{grad} \varphi')_{\mathcal{D}_c} &= 0 \end{aligned} \quad (1)$$

where μ represents the magnetic permeability, σ represents the conductivity, and ω represents the pulsation. \mathbf{A}' and φ' are the test functions. To ensure the uniqueness of the solution, it is necessary to impose a gauge condition on \mathbf{A} and on φ . Now, the domain \mathcal{D} is discretized with a mesh τ_h made of tetrahedra denoted by \mathcal{T} and faces by \mathcal{F} . The discretisation of the weak formulation (1) takes the form

$$\begin{aligned} (\mu^{-1} \mathbf{curl} \mathbf{A}_h, \mathbf{curl} \mathbf{A}'_h)_{\mathcal{D}} + (\sigma (j\omega \mathbf{A}_h + \mathbf{grad} \varphi_h), \mathbf{A}'_h)_{\mathcal{D}_c} \\ = (\mathbf{J}_s, \mathbf{A}'_h)_{\mathcal{D}} \\ (\sigma (j\omega \mathbf{A}_h + \mathbf{grad} \varphi_h), \mathbf{grad} \varphi'_h)_{\mathcal{D}_c} = 0. \end{aligned} \quad (2)$$

Here, the subscript h means that the corresponding functions belong to finite dimensional spaces associated with the mesh τ_h .

Manuscript received June 27, 2017; accepted July 28, 2017. Date of publication August 7, 2017; date of current version February 21, 2018. Corresponding author: F. Piriou (e-mail: francis.piriou@univ-lille1.fr).

Color versions of one or more of the figures in this paper are available online at <http://ieeexplore.ieee.org>.

Digital Object Identifier 10.1109/TMAG.2017.2736601

TABLE I
PROPERTIES OF FIELDS

Properties of fields	Formulations	
	A- φ	T- Ω
$[\mathbf{E}_h \wedge \mathbf{n}]_F = \mathbf{0}$	Strong sense	Weak sense
$[\mathbf{H}_h \wedge \mathbf{n}]_F = \mathbf{0}$	Weak sense	Strong sense
$[\mathbf{B}_h \cdot \mathbf{n}]_F = \mathbf{0}$	Strong sense	Weak sense
$[\mathbf{J}_h \cdot \mathbf{n}]_F = \mathbf{0}$	Weak sense	Strong sense

Notation $[\]_F$ represents the jump on each face F

C. Magnetic Formulation

Another possibility to solve the Maxwell equations in magnetodynamic harmonic is to use the magnetic formulation in term of electric vector potential \mathbf{T} and magnetic scalar potential Ω . Using similar development at the electric formulation [6], the weak formulation can be written

$$\begin{aligned} (\sigma^{-1} \mathbf{curl} \mathbf{T}, \mathbf{curl} \mathbf{T}')_{\mathcal{D}_c} + (j\omega\mu(\mathbf{H}_s + \mathbf{T} - \mathbf{grad}\Omega), \mathbf{T}')_{\mathcal{D}_c} &= 0 \\ (\mu(\mathbf{H}_s + \mathbf{T} - \mathbf{grad}\Omega), \mathbf{grad}\Omega')_{\mathcal{D}_c} &= 0 \\ (\mu(\mathbf{H}_s - \mathbf{grad}\Omega), \mathbf{grad}\Omega')_{\mathcal{D}_{nc} \cup \mathcal{D}_s} &= 0 \end{aligned} \quad (3)$$

where \mathbf{H}_s is a source field so that $\mathbf{curl} \mathbf{H}_s = \mathbf{J}_s$. The discretization of the weak formulation using a mesh made of tetrahedra gives the next discrete form

$$\begin{aligned} (\sigma^{-1} \mathbf{curl} \mathbf{T}_h, \mathbf{curl} \mathbf{T}'_h)_{\mathcal{D}_c} &+ (j\omega\mu(\mathbf{H}_s + \mathbf{T}_h - \mathbf{grad}\Omega_h), \mathbf{T}'_h)_{\mathcal{D}_c} = 0 \\ (\mu(\mathbf{H}_s + \mathbf{T}_h - \mathbf{grad}\Omega_h), \mathbf{grad}\Omega'_h)_{\mathcal{D}_c} &= 0 \\ (\mu(\mathbf{H}_s - \mathbf{grad}\Omega_h), \mathbf{grad}\Omega'_h)_{\mathcal{D}_{nc} \cup \mathcal{D}_s} &= 0 \end{aligned} \quad (4)$$

D. Properties of Fields

According to the used formulation, the properties of fields are verified in strong sense or weak sense. In Table I, these different properties are presented for the numerical solutions of the fields \mathbf{E}_h , \mathbf{H}_h , \mathbf{B}_h , and \mathbf{J}_h .

III. ERROR ESTIMATORS

A. Definition of Reliability and Efficiency

From a mathematical point of view, the reliability and the efficiency properties [3] prove that the estimator is equivalent to the error and justify its use in an adaptive mesh refinement framework. The reliability is defined by

$$\varepsilon \leq C_1 \eta \quad (5)$$

and the efficiency by

$$C_2 \eta_{\mathcal{T}} \leq \varepsilon_{\mathcal{P}(\mathcal{T})} \quad (6)$$

where C_1 and C_2 are two positive constants which only depend on the data of the problem but not on the mesh size h . η and $\eta_{\mathcal{T}}$ are, respectively, the global error estimator and the local

error estimator in the element \mathcal{T} . In the same way, ε and $\varepsilon_{\mathcal{P}(\mathcal{T})}$ represent the global error in the whole domain and the local error in the patch of the element $\mathcal{P}(\mathcal{T})$ [3].

B. Residual Error Estimator

1) *A- φ Formulation:* In the case of **A- φ** formulation the local error estimator on a tetrahedron \mathcal{T} is defined by [7]

$$\eta_{\mathcal{T}}^2 = \eta_{\mathcal{T};1}^2 + \eta_{\mathcal{T};2}^2 + \eta_{\mathcal{T};3}^2 + \sum_{F \subset \partial \mathcal{T}} (\eta_{F;1}^2 + \eta_{F;2}^2) \quad (7)$$

where

$$\eta_{\mathcal{T};1} = h_{\mathcal{T}} \|\mathbf{J}_s - \mathbf{curl}(\mu^{-1} \mathbf{curl} \mathbf{A}_h) - \sigma(j\omega \mathbf{A}_h + \mathbf{grad} \varphi_h)\|_{\mathcal{T}} \quad (8)$$

$$\eta_{\mathcal{T};2} = h_{\mathcal{T}} \|\mathbf{div}(\sigma(j\omega \mathbf{A}_h + \mathbf{grad} \varphi_h))\|_{\mathcal{T}} \quad (9)$$

$$\eta_{\mathcal{T};3} = h_{\mathcal{T}} \|\mathbf{J}_s - \pi_h \mathbf{J}_s\|_{\mathcal{T}} \quad (10)$$

$$\eta_{F;1} = h_F^{1/2} \|[\mathbf{n} \wedge \mu^{-1} \mathbf{curl} \mathbf{A}_h]_F\|_F \quad (11)$$

$$\eta_{F;2} = h_F^{1/2} \|[\sigma(j\omega \mathbf{A}_h + \mathbf{grad} \varphi_h) \cdot \mathbf{n}]_F\|_F. \quad (12)$$

We denote $h_{\mathcal{T}}$ and h_F the diameter of the element and the facet, respectively. Equations (8) and (9) evaluate, for each element, the error on the volumic residual. The expression (10) gives the discretization error of the source term. Finally, (11) and (12) evaluate respectively the jumps of the tangential component of magnetic field \mathbf{H}_h and the jump of the normal component of the induced current density \mathbf{J}_h through a facet between two elements. From the local estimation $\eta_{\mathcal{T}}$ the global error estimation $\eta_{\text{Res A-}\varphi}$ is obtained by a discrete sum on the mesh such as

$$\eta_{\text{Res, A-}\varphi}^2 = \sum_{\mathcal{T} \in \tau_h} \eta_{\mathcal{T}}^2. \quad (13)$$

2) *T- Ω Formulation:* For the **T- Ω** formulation the local error estimator takes a similar form than the **A- φ** formulation and can be written under the form [6], [7]

$$\eta_{\mathcal{T}}^2 = \eta_{\mathcal{T};1}^2 + \eta_{\mathcal{T};2}^2 + \sum_{F \subset \partial \mathcal{T}} (\eta_{F;1}^2 + \eta_{F;2}^2) \quad (14)$$

$$\eta_{\mathcal{T};1} = h_{\mathcal{T}} \|\mathbf{curl}(\sigma^{-1} \mathbf{curl} \mathbf{T}_h) + j\omega\mu \mathbf{H}_h\|_{\mathcal{T}} \quad (15)$$

$$\eta_{\mathcal{T};2} = h_{\mathcal{T}} \|\mathbf{div}(j\omega\mu \mathbf{H}_h)\|_{\mathcal{T}} \quad (16)$$

$$\eta_{F;1} = h_F^{1/2} \|[\mathbf{n} \wedge \sigma^{-1} \mathbf{rot} \mathbf{T}_h]_F\|_{F'} \quad (17)$$

$$\eta_{F;2} = h_F^{1/2} \|[\mu \mathbf{H}_h \cdot \mathbf{n}]_F\|_{F'}. \quad (18)$$

In (15), (16), and (18) the discrete expression of the magnetic field \mathbf{H}_h can be written under the form

$$\mathbf{H}_h = \mathbf{H}_s + \mathbf{T}_h - \mathbf{grad}\Omega_h \quad \text{in } \mathcal{D}_c \quad (19)$$

$$\mathbf{H}_h = \mathbf{H}_s - \mathbf{grad}\Omega_h \quad \text{in } \mathcal{D}_{nc} \cup \mathcal{D}_s. \quad (20)$$

In expressions of the error estimator, (15) and (16) evaluate on each element the error on volumic residual. The expressions (17) and (18) verify, respectively, the jumps of the tangential component of the electric field \mathbf{E}_h and the jumps of the normal component of the magnetic flux density \mathbf{B}_h through a facet of the element. As in the case of the **A- φ** formulation the global error estimation $\eta_{\text{Res T-}\Omega}$ is obtained by a discrete sum of the local error (13) on the mesh.

C. Equilibrated Error Estimator

From the $\mathbf{A}\text{-}\varphi$ formulation solved by a finite-element method, we obtain a pair of admissible fields [5] (magnetic flux density \mathbf{B}_h and electric field \mathbf{E}_h). In the same way the $\mathbf{T}\text{-}\Omega$ formulation gives two admissible fields (\mathbf{J}_h and \mathbf{H}_h). From these fields, and the non-verification of equilibrium equations at the discrete level, we can introduce the magnetic Ligurian [8] which can be extended to the electric one [9]. In these conditions, it is possible to define the local error estimator on a tetrahedron \mathcal{T} so that [5]

$$\eta_{\mathcal{T}\text{-Eq.}}^2 = \|\mu^{1/2}(\mathbf{H}_h - \mu^{-1}\mathbf{B}_h)\|_{\mathcal{T}}^2 + \|(\sigma\omega)^{-1/2}(\mathbf{J}_h - \sigma\mathbf{E}_h)\|_{\mathcal{T}}^2. \quad (21)$$

It can be shown that there is a link between the local estimator and the local error [5]

$$\eta_{\mathcal{T}\text{-Eq.}}^2 \leq 2(\varepsilon_{\mathcal{T}\text{-A-}\varphi}^2 + \varepsilon_{\mathcal{T}\text{-T-}\Omega}^2) \quad (22)$$

where $\varepsilon_{\mathcal{T}\text{-A-}\varphi}$ and $\varepsilon_{\mathcal{T}\text{-T-}\Omega}$ are the errors due to, respectively, $\mathbf{A}\text{-}\varphi$ and $\mathbf{T}\text{-}\Omega$ formulations. As previously from the local estimation $\eta_{\mathcal{T}\text{-Eq.}}$ the global error estimation $\eta_{\text{Eq.}}$ is obtained by a discrete sum on the mesh. As shown in [5], there is a direct link between the estimator and the error so that

$$\eta_{\text{Eq.}}^2 = \sum_{\mathcal{T} \in \tau_h} \eta_{\mathcal{T}\text{-Eq.}}^2. \quad (23)$$

Then obtain

$$\eta_{\text{Eq.}}^2 = (\varepsilon_{\mathbf{A}\text{-}\varphi}^2 + \varepsilon_{\mathbf{T}\text{-}\Omega}^2) \quad (24)$$

up to some higher order terms. In this case, in order to determine the admissible fields, we have used both formulations ($\mathbf{A}\text{-}\varphi$ and $\mathbf{T}\text{-}\Omega$), for this reason, from now, we denote this estimator $\eta_{\text{Eq.dual}}$.

Another solution consists in using the $\mathbf{A}\text{-}\varphi$ formulation to obtain \mathbf{B}_h and \mathbf{E}_h and then to construct locally the two admissible fields \mathbf{J}_h and \mathbf{H}_h [10].

Practically, in order to construct \mathbf{J}_h we use the current density given by the $\mathbf{A}\text{-}\varphi$ formulation denoted $\mathbf{J}_{h,\mathbf{A}\text{-}\varphi}$ which is not with divergence free ($\text{div}\mathbf{J}_{h,\mathbf{A}\text{-}\varphi} \neq 0$). Then we determine \mathbf{J}_h by imposing two conditions. We search the courant densities \mathbf{J}_h which are with divergence free. From the possible solutions $\tilde{\mathbf{J}}_h$ we choose the closest to the current density $\mathbf{J}_{h,\mathbf{A}\text{-}\varphi}$. Consequently, we must verify

$$\|\text{div}\mathbf{J}_h\|_{\mathcal{D}_c} = 0 \text{ and } \mathbf{J}_h = \underset{\tilde{\mathbf{J}}_h}{\text{argmin}} \|(\mathbf{J}_{h,\mathbf{A}\text{-}\varphi} - \tilde{\mathbf{J}}_h)\|_{\mathcal{D}_c}. \quad (25)$$

Afterward the admissible magnetic field \mathbf{H}_h is computed through a classical magnetic scalar potential formulation with source term equal to $\mathbf{J}_{\text{sh}} + \mathbf{J}_h$ [10]. At this step we have two admissible fields ($\mathbf{J}_{h,\mathbf{A}\text{-}\varphi}$ and \mathbf{H}_h) and the local estimator $\eta_{\tau\text{-Eq,Const}}$ can be computed formally as the dual one [see (21)] and the global estimator $\eta_{\text{Eq,Const}}$ as $\eta_{\text{Eq,dual}}$ in (23).

IV. NUMERICAL APPLICATIONS

In order to evaluate the effectiveness of the error estimators a coil between two conductive plates has been studied. The structure and a part of the mesh are presented in Fig. 2.



Fig. 2. Mesh of the studied structure.

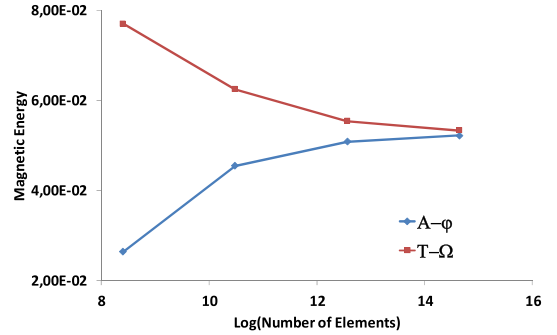


Fig. 3. Evolution of the magnetic energy for different meshes.

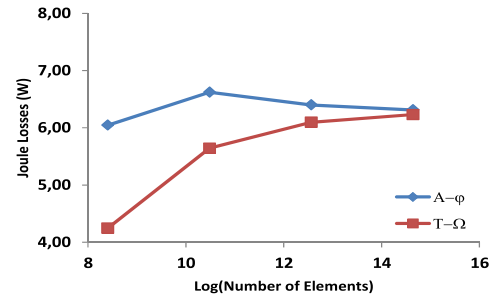


Fig. 4. Evolution of Joule losses for different meshes.

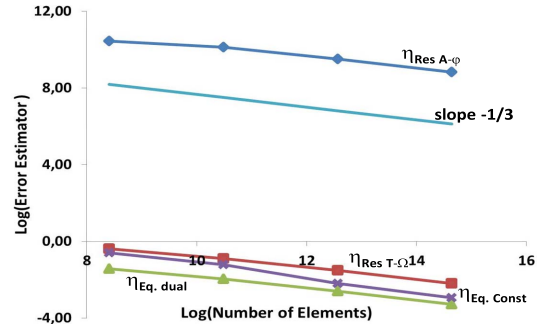


Fig. 5. Comparison of residual and equilibrated estimators.

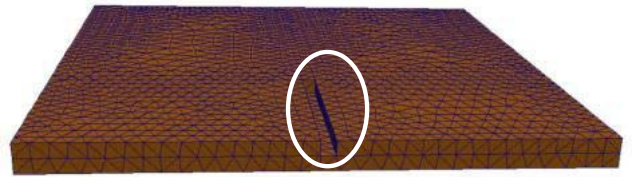


Fig. 6. Mesh of the below plate with a groove.

In the first step the coil is fed by a sinusoidal current of 1 A at the frequency of 50 Hz. To compare the error estimators four regular meshes have been used between 4500 and 229000 elements.

For the different meshes, Fig. 3 shows the evolution of the magnetic energy in the whole domain obtained by both ($\mathbf{A}\text{-}\varphi$) and $\mathbf{T}\text{-}\Omega$) formulations. In the same way, Fig. 4 shows the power losses in the plates. From these figures, we observe the convergence of the global quantities with respect to the number of elements.

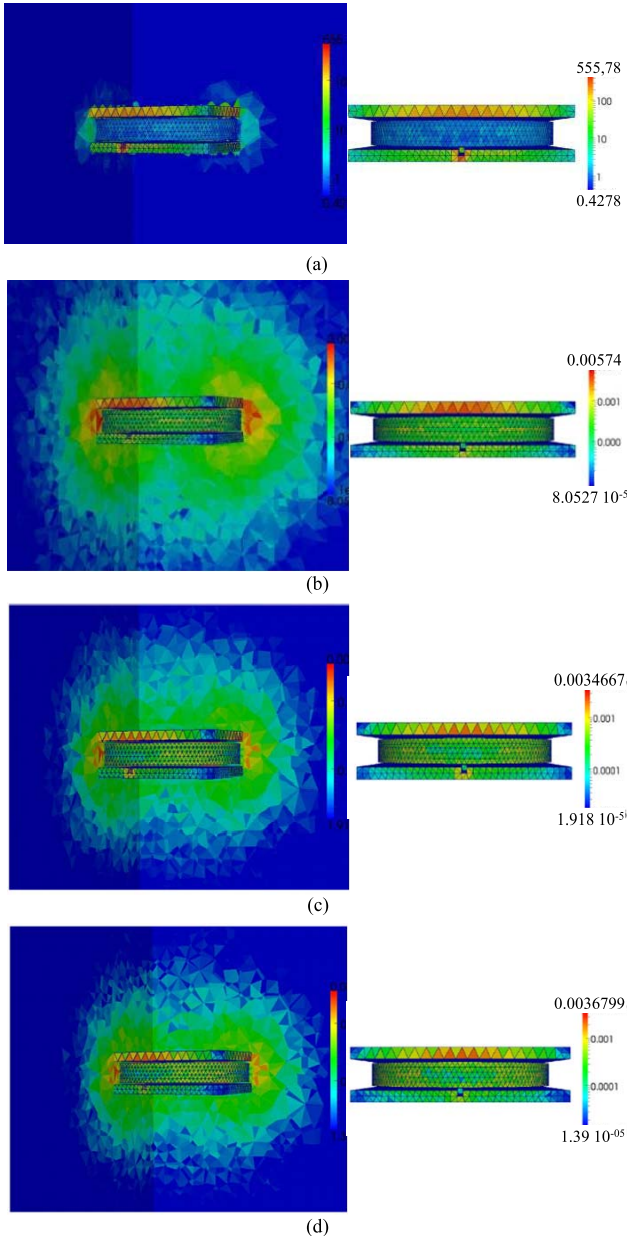


Fig. 7. Local error estimator maps. (a) $\eta_{\text{Res } A-\varphi}$. (b) $\eta_{\text{Res } T-\Omega}$. (c) $\eta_{\text{Eq, dual}}$. (d) $\eta_{\text{Eq, Const}}$.

To compare the proposed estimators, Fig. 5 shows the evolution of the error estimators as a function of the meshes. We observe that all the estimators have a slope a little bit less of $-1/3$ which is the reference in finite elements for regular solutions. Fig. 5 also shows that the results of both equilibrated estimators $\eta_{\text{Eq, dual}}$ and $\eta_{\text{Eq, Const}}$ are similar. Conversely, due to the unknown constants in (5) and (6) for the residual estimators ($\eta_{\text{Res } A-\varphi}$ and $\eta_{\text{Res } T-\Omega}$) the results are distant from the equilibrated estimators. Nevertheless, the estimator $\eta_{\text{Res } T-\Omega}$ gives some results near both equilibrated estimators.

In order to analyze the behavior of the estimators in the presence of a perturbation on the current density, a groove of square cross section is realized in the middle of the plate located below the coil (see Fig. 6).

Calculations were made using the $A-\varphi$ and $T-\Omega$ formulations. In Fig. 7, we show the error maps obtained with the four

estimators. In the left, we have the studied structure and in the right, a focus on the coil and the two plates. Fig. 7(a) displays the error map of the $A-\varphi$ formulation given by the residual error estimator ($\eta_{\text{Res, } A-\varphi}$). From Fig. 7, we observe that the error is more important in the plates and more particularly near the groove. This observation complies with the properties of fields given in Table I. Conversely, as expected, in Fig. 7(b), which displays the residual error map corresponding to the $T-\Omega$ formulation, the error is not extremely important near the groove.

At last for the equilibrated error estimators, [Fig. 7(c) and (d)] the error maps are similar. On the other hand, if we look at the maximum values of the error maps, it can be noted that for the balanced estimators they are very close. For the residual estimators they are different because of the constant C_2 in (6). In fact we find similar results as those given in Fig. 5.

V. CONCLUSION

In conclusion, two families of error estimators are studied for classical formulations of harmonic eddy-current problems. For a given structure, comparisons are done as a function of regularly refined meshes and the proposed estimators are in good agreement with the expected convergence behavior. Moreover, the analysis of error maps for the proposed estimators is done and discussed. The obtained results are in good agreement with the theoretical developments. In the continuation to complete this analysis the equilibrated error estimator will be developed for $T-\Omega$ formulation.

REFERENCES

- [1] R. Beck, R. Hiptmair, R. H. Hoppe, and B. Wohlmuth, "Residual based a posteriori error estimators for eddy current computation," *ESAIM, Math. Modell. Numer. Anal.*, vol. 34, no. 1, pp. 159–182, 2000.
- [2] R. Verfürth, *A Review of a Posteriori Error Estimation and Adaptive Mesh-Refinement Techniques*. New York, NY, USA: Wiley, 1996.
- [3] M. Ainsworth and J. T. Oden, *A Posteriori Error Estimation in Finite Element Analysis*. New York, NY, USA: Wiley, 2000.
- [4] Z. Tang, Y. Le Menach, E. Creusé, S. Nicaise, F. Piriou, and N. Némitz, "Residual based a posteriori error estimators for harmonic A/φ and T/Ω formulations in eddy current problems," *IEEE Trans. Magn.*, vol. 49, no. 5, pp. 1721–1724, May 2013.
- [5] E. Creusé, S. Nicaise, and R. Tittarelli, "A guaranteed equilibrated error estimator for the $A-\varphi$ and $T-\Omega$ magnetodynamic harmonic formulations of the Maxwell system," *IMA J. Numer. Anal.*, vol. 37, no. 2, pp. 750–773, 2016, doi: 10.1093/imanum/drw026.
- [6] Z. Tang, Y. Le Menach, E. Creusé, S. Nicaise, F. Piriou, and N. Némitz, "A posteriori residual error estimators with mixed boundary conditions for quasi-static electromagnetic problems," *COMPEL, Int. J. Comput. Math. Elect. Electron. Eng.*, vol. 34, no. 3, pp. 724–739, 2015.
- [7] E. Creusé, S. Nicaise, Z. Tang, Y. Le Menach, N. Némitz, and F. Piriou, "Residual-based a posteriori estimators for the $A-\varphi$ magnetodynamic harmonic formulation of the Maxwell system," *Math. Mod. Methods Appl. Sci.*, vol. 22, no. 5, p. 30, 2012.
- [8] J. Rikabi, C. F. Bryant, and E. M. Freeman, "An error-based approach to complementary formulations of static field solutions," *Int. J. Numer. Methods Eng.*, vol. 26, no. 9, pp. 1963–1987, Sep. 2005.
- [9] C. Li, Z. Ren, and A. Razek, "An approach to adaptive mesh refinement for three-dimensional eddy-current computations," *IEEE Trans. Magn.*, vol. 30, no. 1, pp. 113–117, Jan. 1994.
- [10] R. Tittarelli, Y. Le Menach, F. Piriou, E. Creusé, S. Nicaise, and J. P. Ducreux, "A guaranteed equilibrated error estimator for the harmonic $A-\varphi$ formulation in eddy current problems," in *Proc. CEFC*, Miami, FL, USA, Nov. 2016, p. 1.